Proceedings of the 9th World Congress on Electrical Engineering and Computer Systems and Sciences (EECSS'23)
Brunel University, London, United Kingdom – August 03-05, 2023
Paper No. ICBES 119
DOI: 10.11159/icbes223.119

Workflow and Clinical Implementation of a Simulation Method for the Analysis of Hemodynamics and Structural Mechanics of Cerebral Aneurysms

Jozsef Nagy[1], Matthias Gmeiner[2], Veronika Miron[3], Julia Maier[3], Wolfgang Fenz[4], Zoltan Major[3], Andreas Gruber[2]
[1]eulerian-solutions e.U.
Leonfeldnerstraße 245, Linz, Austria
jozsef.nagy@eulrian.solutions.com
[2]Johannes Kepler University Linz - Universitätsklinik für Neurochirurgie
Wagner-Jauregg-Weg 15, Linz, Austria
matthias.gmeiner@kepleruniklinikum.at; andreas.gruber_1@kepleruniklinikum.at
[3]Johannes Kepler University Linz - Institute of Polymer Product Engineering
Altenberger Strasse 69, Linz, Austria
veronika.miron@jku.at; julia.maier@jku.at; zoltan.major@jku.at
[4] RISC Software GmbH
Softwarepark 32a, Hagenberg, Austria
wolfgang.fenz@risc-software.at

Abstract **–** The treatment of patients with cerebral aneurysms poses multiple challenges to physicians from rupture to treatment risk assessment and their consequences to the patient's health. Risk estimation support is highly required to make the optimum decisions for individual patients. The aim of this study is to develop the workflow of a simulation method for the analysis of hemodynamics and structural mechanics of cerebral aneurysms as well as its possible clinical implementation.
Medical imaging data was taken and converted into CAD data (STL format) to use as geometric input for simulations. Fluid-Structure Interaction (FSI) simulations are utilized in the inflow vessel, the outflow vessels as well as a typical aneurysm. Aitken's underrelaxation method is used to ensure convergence between hemodynamics and structural mechanics. The influence of linear and non-linear elastic material properties of the vessel wall as well as the influence of wall thickness reduction in the aneurysm sac are investigated.
In this work, two major hemodynamic (wall shear stress and oscillatory shear index) and two structural mechanic quantities (wall displacement and Mises stress) are evaluated and compared between the different models. The linear elastic material model tends to overestimate displacements at high strain rates. The reduction of wall thickness in the aneurysm region shows an increase in wall stresses. In both cases hemodynamic phenomena are not changed, however a tendency of aneurysm growth can be identified.
The model is implemented as part of a graphical user interface. With this, it is possible for medical personnel without simulation background to run sophisticated Fluid-Structure interaction simulations with ease and in future to make optimized decisions for patient treatment.

Keywords**:** cerebral aneurysm, hemodynamics, structural mechanics, fluid-structure interaction, visualization

1. Introduction

Cerebral aneurysms are occurring in about 2–5% of the overall population [1]. Rupture of aneurysms lead to subarachnoid hemorrhage (SAH), which is commonly associated with high mortality and morbidity. Several studies have demonstrated various well-known clinical, genetic, morphological or hemodynamic factors for initiation, growth and rupture of cerebral aneurysms [2,3,4].

An increase in the use of medical imaging has led to a larger number of detected unruptured aneurysms. This in turn leads to an increased need for treatment decisions. Only aneurysms close to rupture should be treated as the treatment itself contains many risks for the patient. Thus reliable support for decision making is needed to better treat patients.

Recently, investigations using computational fluid dynamics (CFD) could demonstrate significantly different hemodynamics in ruptured versus unruptured aneurysms [5,6,7]. Hemodynamic phenomena provide mechanical triggers that are transduced into biological signals leading to possible aneurysm growth and rupture [8]. Hemodynamics are influenced by aneurysm geometry and thus morphological parameters [9].

Further, although many detailed fluid dynamics simulations including complex flow patterns have been performed [2,3,5,6,7,8,9,10], so far only a few studies have focused on structural dynamics calculations [11,12,13]. In our opinion, a comprehensive evaluation of individual hemodynamics should include analysis of fluid as well as structural aspects using fluid-structure interaction (FSI) analysis.

To model combined hemodynamics as well as structural mechanics, a reliable simulation workflow is developed and implemented into a simulation suite. This way in the future medical personnel can also set up, start, and evaluate simulations without extensive simulation background.

2. Methods

2.1. Patient image data, simulation geometry and mesh

The aneurysm geometry is extracted from medical image data obtained via digital subtraction angiography (DSA). The segmentation of the cerebral aneurysm geometry is performed with intensity thresholding and minor editing of the voxel volume. The segmentation is converted into a surface mesh via the marching cubes algorithm. The centerline of the surface mesh is calculated and inlet as well as outlet planes are placed perpendicular to these lines. The final set of surfaces (vessel, aneurysm, inflow, outflow) is saved as STL files (see figure 1 left).

The volumetric fluid mesh is automatically generated utilizing the STL files as input. The solid mesh is extruded from the fluid mesh with a certain pre-defined thickness. Figure 1 shows on the right-hand side a typical calculation mesh in the fluid (grey) and solid (red) region.

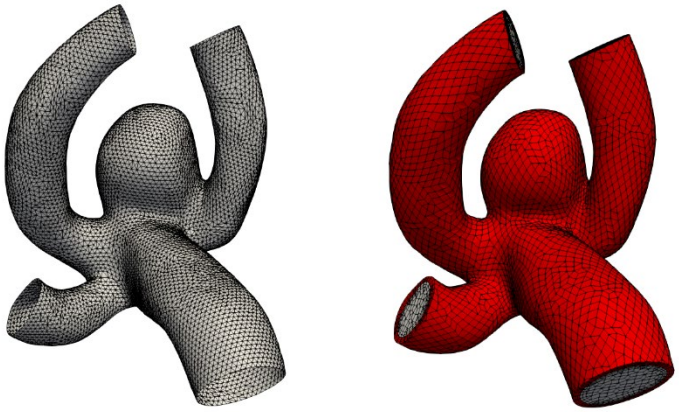

Fig. 1: Generated STL file of aneurysm (left) and generated volume mesh for simulations (right)

2.2. Hemodynamic and structural mechanic modelling

An in-house finite volume solver based on the open-source computational fluid dynamics tool OpenFOAM [13] in combination with the fluid-structure interaction library solids4Foam [14] was used to numerically solve the unsteady equations of the process.

For hemodynamic modelling the governing equations are given by the principles of mass and momentum conservation with the help of the continuity equation as well as the Navier Stokes equations,

$$\frac{\partial \rho}{\partial t} + \nabla \cdot \rho \mathbf{u} = 0 \tag{1}$$

$$\frac{\partial \rho \mathbf{u}}{\partial t} + \nabla \cdot \rho \mathbf{u}\mathbf{u} = -\nabla p + \boldsymbol{\nabla} \cdot \boldsymbol{\sigma} + \mathbf{F} \tag{2}$$

Here, ρ is the fluid density, t is the time, $\mathbf{u}$ is the velocity vector, p is the fluid pressure, $\boldsymbol{\sigma}$ is the fluid stress tensor and $\mathbf{F}$ is the vector of possibly additional forces (e.g. gravitation). In order to analyse hemodynamic results, the oscillatory shear index is defined as

$$OSI = \frac{1}{2}\left(1 - \frac{\left\| \int_0^T \boldsymbol{\sigma}_\mathbf{W}\, dt \right\|}{\int_0^T \|\boldsymbol{\sigma}_\mathbf{W}\|\, dt}\right) \tag{10}$$

where, σ_s is the fluid wall shear stress (WSS) vector. The index is defined in the interval between [0;0.5] and gives the quantity of oscillatory behaviour of the wall shear stress on the fluid wall.

For structural mechanic modelling, the principle of force conservation is utilized. For linear elastic materials the equation is given by

$$\int_{\Omega_0} \frac{\partial^2 \rho_s \mathbf{u}_s}{\partial t^2} d\Omega_0 = \oint_{\Gamma_0} \mathbf{n_0} \cdot \boldsymbol{\sigma_s} d\Gamma_0 + \int_{\Omega_0} \rho_s \mathbf{b}\, d\Omega_0 \tag{3}$$

$$\boldsymbol{\sigma_s} = 2\mu \boldsymbol{\varepsilon_s} + \lambda\, tr(\boldsymbol{\varepsilon_s})\, I \tag{4}$$

$$\boldsymbol{\varepsilon_s} = \frac{1}{2}\left(\boldsymbol{\nabla}\mathbf{u}_s + \boldsymbol{\nabla}\mathbf{u}_s{}^T\right) \tag{5}$$

$$\mu = \frac{E}{2(1+\nu)} \tag{6}$$

$$\lambda = \frac{\nu E}{(1+\nu)(1-2\nu)} \tag{7}$$

Here, ρ_s is the solid density, $\mathbf{u}_s$ is the vector of displacement, $\mathbf{n_0}$ is the surface normal vector, $\boldsymbol{\sigma_s}$ is the solid stress tensor and $\mathbf{b}$ is the vector of possible body forces. E is Young's modulus and ν is Poisson's ratio. For non-linear elastic materials equation (3) turns into

$$\int_{\Omega_0} \frac{\partial^2 \rho_s \mathbf{u}_s}{\partial t^2} d\Omega_0 = \oint_{\Gamma_0} (J\mathbf{F}^{-\mathbf{T}} \cdot \mathbf{n_0}) \cdot \boldsymbol{\sigma_s} d\Gamma_0 + \int_{\Omega_0} \rho_s \mathbf{b}\, d\Omega_0 \tag{8}$$

$\mathbf{F}$ is the tensor of the deformation gradient and J is its Jacobian. The stress tensor $\boldsymbol{\sigma_s}$ for non-linear elastic materials is derived from the strain energy function [15]. For the investigated N=3 Ogden model the function is given by

$$W = \sum_{i=1}^{3} \frac{2\mu_i}{\alpha_i^2}\left(\underline{\lambda}_1^{\alpha_i} + \underline{\lambda}_2^{\alpha_i} + \underline{\lambda}_3^{\alpha_i} - 3\right) + \frac{K_1}{2}(J-1)^2 \tag{9}$$

The solution workflow in Fluid-Structure interaction simulations is shown in figure 2 (a). Equations (1)-(9) are solved sequentially by first solving the fluid mechanic equations (1) and (2). Fluid pressure and the stress tensor are interpolated via the interaction surface from fluid to solid. These quantities are added to equations (3) or (8) as body forces. After solving the solid equations (3) or (8), the displacement of the solid is interpolated onto the fluid and the region is morphed accordingly. This workflow is iterated utilizing the Aitken [14] underrelaxation method to guarantee convergence within a time step.

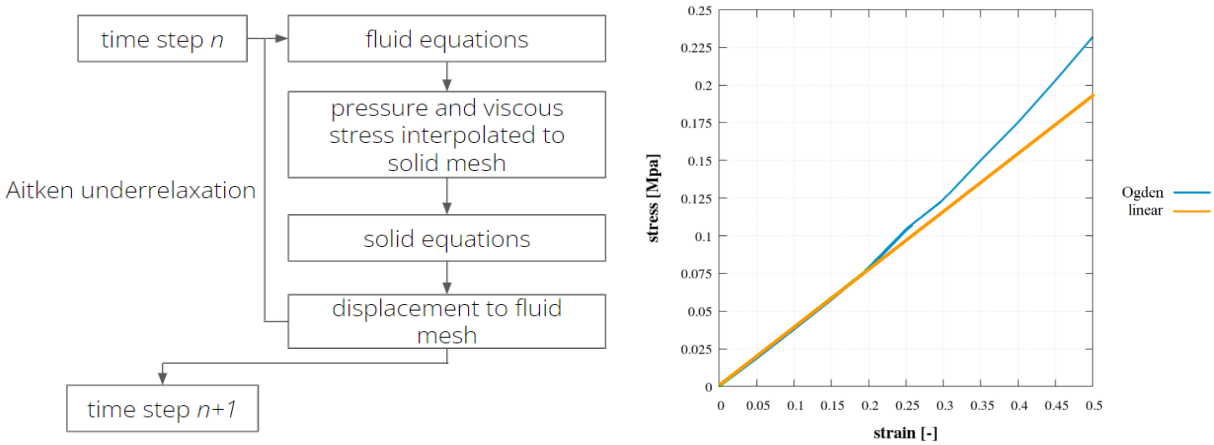

(a) (b)

Fig. 2: Fluid-Structure Interaction iteration workflow within a time step (a) and utilized stress-strain curve for the linear and non-linear models (b)

A pulsatile flow condition in the form of a time-dependent velocity curve [16] is imposed as boundary conditions for the fluid flow at the inflow surface, whereas experimental pressure data is taken from [17] in order to define a time dependent condition at the outflow surface. Along the walls no-slip conditions are assumed. Blood is modelled as a fluid with a viscosity of 0.04 Poise and a density of 1.06 g/cm^3. One cardiac cycle [18] with a heart-beat rate of 60 beats per minute is calculated with 100 time steps per cardiac cycle.

Solid mechanic boundary conditions are applied by fixing the vessel walls at the in- and outflow faces. The vessel wall is assumed to be either linear or nonlinear elastic. For linear elastic modelling, a Young's modulus value of 24.9 MPa [18] and a Poisson's ratio of 0.49 are utilized. In the non-linear elastic simulations with the Ogden model constants are set to be $\mu_1 = 0.65e6, \mu_2 = \mu_3 = 0,$ and $\alpha_1 = 4.84, \alpha_2 = \alpha_3 = 1$. Figure 2 (b) shows the strain-stress curve for the linear and non-linear elastic material model. A deviation between the curves above a strain of 0.2 can be clearly seen, where at high stress values the strain (and displacement) is overestimated by the linear elastic model.

3. Hemodynamic and structural mechanic behaviour

3.1. Influence of linear and non-linear material model

Figure 3 shows the relative wall shear stress (WSS scaled by the maximum value) as well as the oscillatory shear index (OSI) for the linear and non-linear elastic material models. WSS is high in the parent vessel and is low in the aneurysm. In contrast OSI is high in the aneurysm, which may indicate aneurysm growth [8]. Comparing the linear and non-linear elastic simulations no significant difference can be seen in the hemodynamic quantities, as the difference is in the structural modelling.

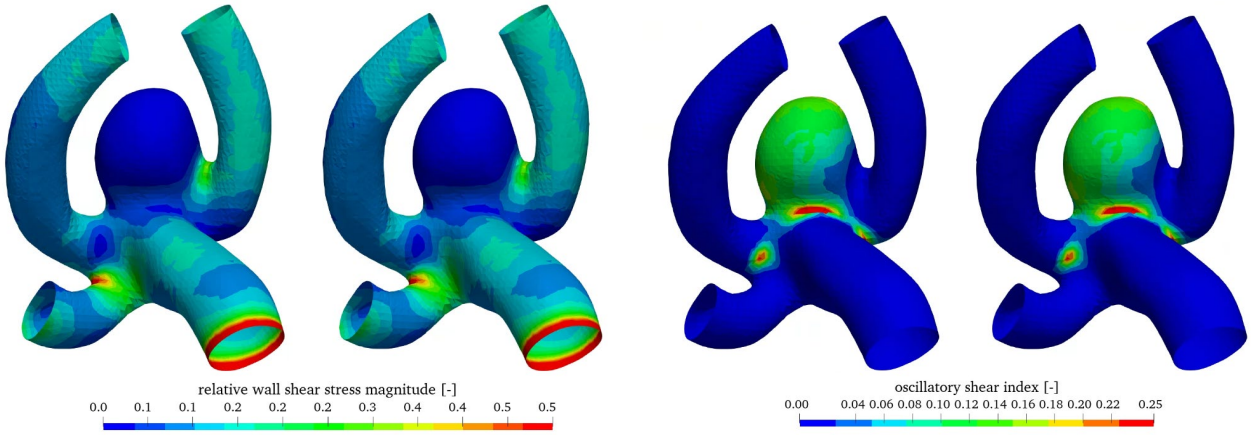

(a) **(b)**

Fig. 3: Wall shear stress (a) and oscillatory shear index (b) with the linear (left aneurysm) and the non-linear elastic model (right aneurysm)

Figure 4 shows the wall displacement as well as the wall equivalent Mises stress. As expected from figure 2 (b) the displacement is overestimated by the linear elastic material model especially in the aneurysm sac. The stress distribution is slightly elevated in the case of the non-linear elastic model, however the qualitative distribution is very similar.

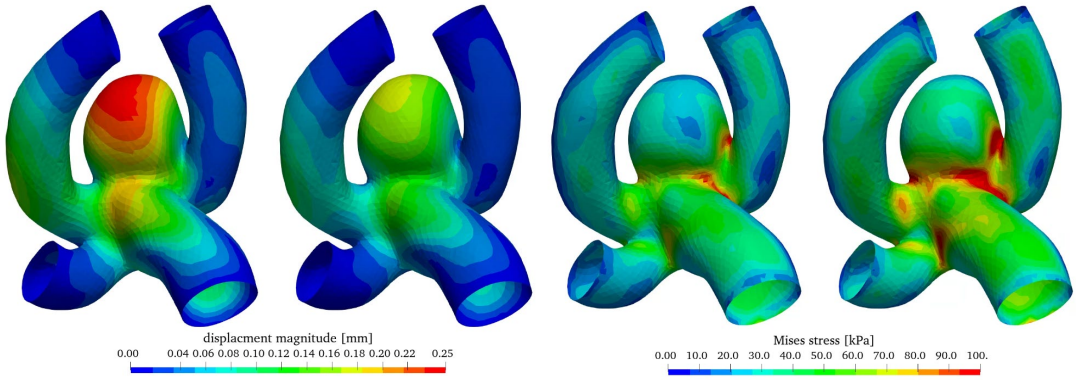

(a) **(b)**

Fig. 4: Wall displacement (a) and Mises stress (b) with the linear (left aneurysm) and the non-linear elastic model (right aneurysm)

The linear elastic model is adequately accurate for stress estimations, however for high stress/strain scenarios only the non-linear elastic model can be utilized for displacement estimation.

3.2. Influence of wall thickness

In addition, the workflow also enables the variation of the thickness of the aneurysm wall compared to the parent vessel. Here, the wall thickness of 0.3 mm is reduced to 0.15 mm in the aneurysm wall. The wall thickness in the parent vessel is kept at 0.3 mm. Results compared to the constant wall thickness of 0.3 mm are shown in figure 5, where the relative wall shear stress as well as the oscillatory shear index (OSI) can be seen (both models utilize the linear elastic material model).

Relative WSS and OSI show very similar behaviour in this comparison. The influence of wall thickness reduction is almost negligible.

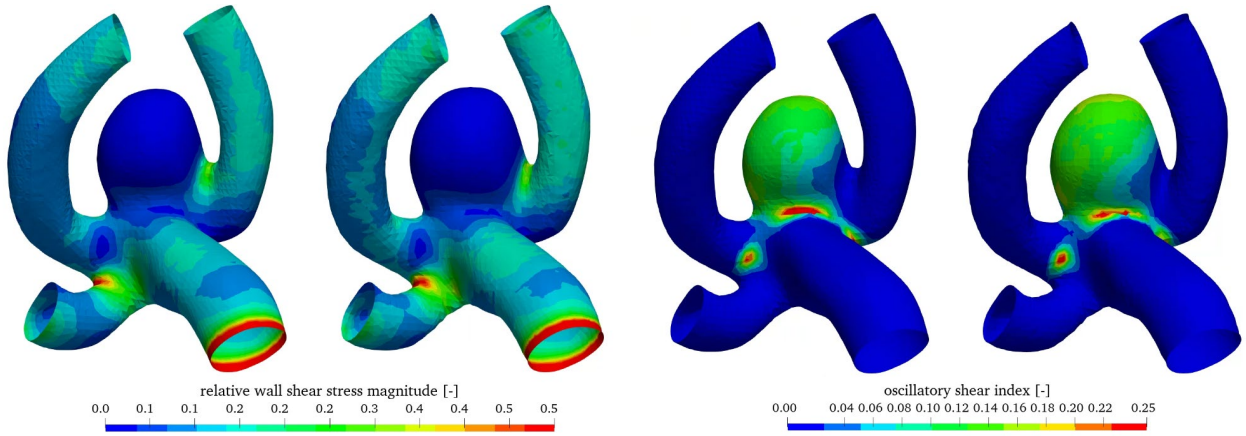

(a) **(b)**

Fig. 5: Wall shear stress (a) and oscillatory shear index (b) with constant (left aneurysm) and varying wall thickness (right aneurysm)

Figure 6 shows the wall displacement as well as the wall equivalent Mises stress with constant and varying wall thickness. A reduction of wall thickness in the aneurysm considerably increases the stress in the wall increasing the potential risk for rupture. Therefore, the wall displacement is also increased.

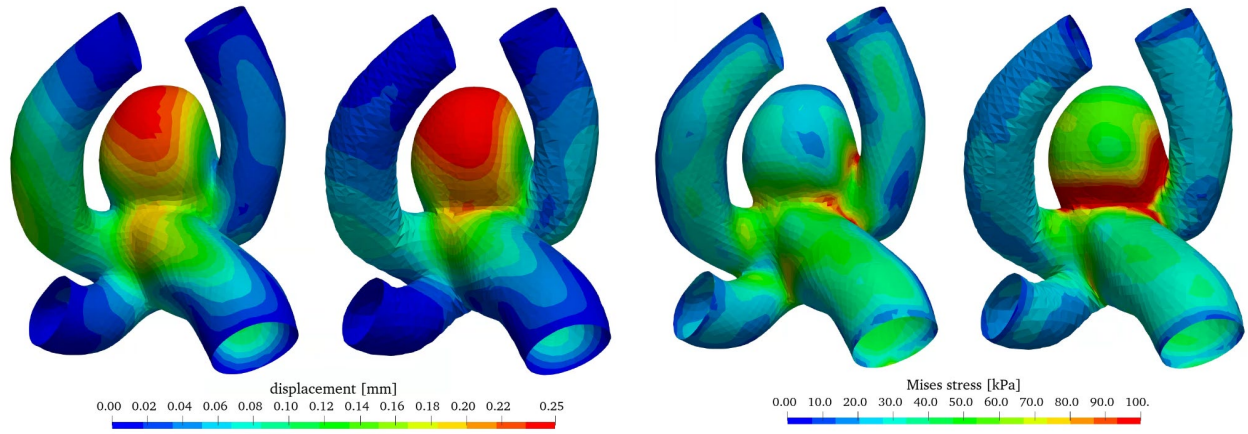

(a) **(b)**

Fig. 6: Wall displacement (a) and Mises stress (b) with constant (left aneurysm) and varying wall thickness (right aneurysm)

With this additional option an even better estimation of rupture behaviour can be achieved in future simulations, by using the most realistic thickness distribution [9].

4. Method implementation for clinical considerations

The presented workflow and results will be used for future clinical considerations of patients with unruptured cerebral aneurysms. Therefore, a software suite has been created for qualitative and quantitative interpretation of hemodynamics as well as structural mechanics.

With the help of a graphical interface, even users without detailed simulation background can set up and start simulations automatically. Figure 7 shows the initial step of medical image segmentation as well as result visualization within the graphical user interface.

Fig. 7: Initial segmentation step (left) and final evaluation step (right) within the implemented GUI

Results can be visualized and qualitatively analysed for focal changes of hemodynamic and structural mechanic quantities. This enables medical personnel to identify low WSS and high OSI regions, which show increased tendencies for aneurysm growth. With the GUI, simulations can be run for annually generated medical data, and a patient history can be created. In case significant changes occur over years, adequate steps can be taken in the treatment of the patient.

In addition, data of over 400 patients will be processed in a future step and simulations will be run. With this it is possible to create a statistical evaluation of hemodynamic and structural mechanic quantities. This way ruptured aneurysms can be statistically compared to stable aneurysms and statistically relevant quantities can be identified, which can be used for rupture risk estimation.

From a clinical point of view, technical advances that allow routine rupture risk prediction in patients with unruptured cerebral aneurysms are highly warranted. Most importantly, this software should be "self-explaining" so that the neurosurgeon can easily use it in his daily routine.

4. Conclusion

In this work a simulation method is presented to model the combined FSI behaviour of hemodynamics and structural mechanics of cerebral aneurysms. Using this method, the analysis of the local distribution of different quantities is possible. Furthermore, clinically relevant behaviour like aneurysm growth or rupture may be estimated.

For rupture estimation, in future steps a statistic evaluation of image data over 400 patients will be conducted to identify statistically significant quantities, which can help separate ruptured (or close to rupture) aneurysms from stable aneurysms.

An intuitive GUI is being developed for medical personnel (especially neurosurgeons) without special simulation background to automatically run simulations and evaluate results.

Acknowledgements

This work was generated in the projects financed by research subsidies granted by the government of Upper Austria and funded by the FFG (Austrian Research Promotion Agency) under the grant 872604 (MEDUSA) and FO999895610 (ARES).

References

[1] S. Dhar, M. Tremmel, J. Mocco, M. Kim, J. Yamasolo, A . H. Siddiqui, L. N. Hopkins and H. Meng, "Morphology Parameters for Aneurysm Rupture Risk Assessment" *Neurosurgery*, vol. 63, no. 2, pp. 185-197, 2008.

[2] S. Jirjees, Z. M. Htun, I.. Aldawudi, P. C. Patwal and S. Khan, "*Role of Morphological and Hemodyanmic Factors in Predicting Intracranial Aneurysm Rutpure: A Review*" *Cureus*, vol. 12, no. 7: e9178, 2020.

[3] H. Meng, V.M. Tutino, J. Xiang, and A. Siddiqui: "*High WSS or Low WSS? Complex Interactions of Hemodynamics with Intracranial Aneurysm Initiation, Growth, and Rupture: Toward a Unifying Hypothesis*" *AJNR Am. J. Neuroradiol.*, vol. 35, no. 7, pp. 1254-1262, 2014.

[4] Japan Investigators UCAS, A. Morita, T. Kirino, K. Hashi, N. Aoki, S. Fukuhara, N. Hashimoto, T. Nakayama, M. Sakai, A. Teramoto, S. Tominari and T. Yoshimoto, "*The natural course of unruptured cerebral aneurysms in a Japanese cohort*". N Engl J Med, vol. 366, pp. 2474- 2482, 2012.

[5] P. Jiang, Q. Liu, J. Wu, X. Chen, M. Li, Z. Li, S. Yang, R. Guo, B. Gao, Y. Cao and S. Wang, "*A Novel Scoring System for Rupture Risk Stratification of Intracranial Aneurysms: A Hemodynamic and Morphological Study*". Front. Neurosci. vol. 12, no. 596, 2018.

[6] F.J. Detmer, B.J. Chung, F. Mut, M. Slawski, F. Hamzei-Sichani, C. Putman, C. Jimenez and J.R. Cebral, "*Development and internal validation of an aneurysm rupture probability model based on patient characteristics and aneurysm location, morphology, and hemodynamics*". Int J CARS, vol. 13, pp. 1767–1779, 2018.

[7] F.J. Detmer, B.J. Chung, F. Mut, M. Slawski, F. Hamzei-Sichani, C. Putman, C. Jimenez and J.R. Cebral, "*Development of a statistical model for discrimination of rupture status in posterior communicating artery aneurysms*". Acta Neurochir, vol. 160, pp. 1643–1652, 2018.

[8] S. Soldozy, P. Norat, M. Elsarrag, A. Chatrath, J.S. Costello, J.D. Sokolowski, P. Tvrdik, M.Y.S. Kalani and M.S. Park. "*The biophysical role of hemodynamics in the pathogenesis of cerebral aneurysm formation and rupture*". Neurosurg Focus. Vol. 47, no. 1, pp. E11. 2019.

[9] J. M. Acosta, A. F. Cayron, N. Dupuy, G. Pelli, B. Foglia, J. Haemmerli, E. Allermann, P. Bijlenga, B. R. Kwak and S. Morel, "*Effect of Aneurysm and Patient Characteristics on Intracranial Aneurysm Wall Thickness*", FRONT CARDIOVASC MED, vol. 8, Article 775307, 2021

[10] J.R. Cebral, F. Mut, D. Sforza, R. Löhner, E. Scrivano, P. Lylyk, C. Putman, "*Clinical application of image-based CFD for cerebral aneurysms*". Int. j. numer. method. biomed. eng., vol. 27, pp. 977–992, 2011.

[11] T.C. Gasser, M. Auer, F. Labruto, J. Swedenborg, J. Roy, „*Biomechanical rupture risk assessment of abdominal aortic aneurysms: Model complexity versus predictability of finite element simulations*". Eur. J. Vasc. Endovasc. Surg., vol. 40, pp. 176–185, 2010.

[12] C. Reeps, M. Gee, A. Maier, M. Gurdan, H.H. Eckstein and W.A. Wall, "*The impact of model assumptions on results of computational mechanics in abdominal aortic aneurysm*", J. Vasc. Surg., vol. 51, pp. 679–688, 2010.

[13] H.G. Weller, G. Tabor, H. Jasak, and C. Fureby. "*A tensorial approach to computational continuum mechanics using object orientated techniques*", Comput. phys., vol. 12, no. 6, pp. 620 – 631, 1998.

[14] P. Cardiff, A. Karač, P. De Jaeger, H. Jasak , J. Nagy, A. Ivanković and Ž. Tuković: "*An open-source finite volume toolbox for solid mechanics and fluid-solid interaction simulations*", arXiv:1808.10736v2, 2018, available at https://arxiv.org/abs/1808.10736

[15] J. T. Oden, *Mechanics of Elastic Structures*, New York, McGraw-Hill, 1967.

[16] P. Blanco, L. Müller and J. David Spence: "*Blood pressure gradients in cerebral arteries: a clue to pathogenesis of cerebral small vessel disease*", Stroke Vasc. Neurol., vol. 2, no. 3, pp. 108-117, 2017.

[17] F. Lorenzetti, S. Suominen and E. Tukianen, "*Evaluation of Blood Flow in Free Microvascular Flaps*", J. Reconstr. Microsurg. Open, vol. 17, no. 3, pp. 163-167, 2001.

[18] B. K. Toth, "*The mechanical interaction between the red blood cells and the blood vessels*", Ph.D. dissertation, University of Budapest, 2011.